Paxinos, G., & Watson, C. (1986) *Stereotaxic Coordinates*, 2nd ed., Academic Press, New York.
Pease, J. H. B., & Wemmer, D. E. (1988) *Biochemistry 27*, 8491-8498.
Schweitz, H., Stansfeld, C. E., Bidard, J.-N., Fagni, L., Maes, P., & Lazdunski, M. (1989) *FEBS Lett. 250*, 519-522.
Seagar, M. J., Labbé-Jullié, C., Granier, C., Goll, A., Glossmann, H., Van Rietschoten, J., & Couraud, F. (1986) *Biochemistry 25*, 4051-4057.
Shipolini, R. (1967) *Chem. Commun. 249*, 6479-6480.
Smith, C., Phillips, M., & Miller, C. (1986) *J. Biol. Chem. 261*, 14607-14613.
Strong, P. N. (1990) *Pharmacol. Ther. 46*, 137-162.
Stühmer, W., Ruppersberg, J. P., Schröter, K. H., Sakmann, B., Stocker, M., Giese, K. P., Perschke, A., Baumann, A., & Pongs, O. (1989) *EMBO J. 8*, 3235-3244.
Toi, K., Bynum, E., Norris, E., & Itano, H. A. (1967), *J. Biol. Chem. 242*, 1036-1043.
Vincent, J.-P., Schweitz, H., & Lazdunski, M. (1975) *Biochemistry 14*, 2521-2525.

# Solution Structure of the Lipophosphoglycan of *Leishmania donovani*†

S. W. Homans,*,‡ A. Mehlert,‡ and S. J. Turco§

*Department of Biochemistry, University of Dundee, Dundee DD1 4HN, Scotland, U.K., and Department of Biochemistry, University of Kentucky Medical Center, Lexington, Kentucky 40536*

*Received May 16, 1991; Revised Manuscript Received October 10, 1991*

ABSTRACT: The three-dimensional solution structure of the repeating $-PO_4-6Gal\beta1-4Man\alpha1-$ disaccharide fragment of the lipophosphoglycan (LPG) derived from *Leishmania donovani* has been determined by use of a combination of homo- and heteronuclear NMR spin coupling constant measurements together with restrained molecular mechanical minimization and molecular dynamics simulations. The fragment exists with limited mobility in solution about the Gal$\beta$1-4Man linkages, whereas in contrast a variety of stable rotamers exist about the Man$\alpha$1-$PO_4$-6Gal linkages. These rotamers define several major stable conformers in solution, which are discussed in terms of the proposed biological role of LPG.

The trypanosomatid *Leishmania donovani* is the etiologic agent of kala azar. It proliferates in hydrolytic environments throughout its digenetic life cycle: as an extracellular promastigote in the alimentary canal of its sandfly vector and as an intracellular amastigote within the phagolysosomes of mammalian macrophages. A major cell surface component of *L. donovani* is a unique glycoconjugate called lipophosphoglycan (LPG) (King et al., 1987). Structurally, the *L. donovani* LPG is a polymer of repeating phosphorylated disaccharide units (on average 16 repeats) of $PO_4$-6Gal$\beta$1-4Man$\alpha$1 linked via a hexasaccharide carbohydrate core to a lyso-1-*O*-alkylphosphatidylinositol lipid anchor (Orlandi & Turco, 1987; Turco et al., 1987, 1989). A similar but immunologically distinct glycoconjugate has been reported in all species of *Leishmania* (Hernandez, 1983; Handman et al., 1984; Handman & Goding, 1984; McConville et al., 1987, 1990). LPG has been reported to bind $Ca^{2+}$ (Eilam et al., 1985) and the biological significance of this is unknown.

The three-dimensional structures of the LPGs from *Leishmania* species are of potential importance since they may help to explain the multiple functions that have been proposed [reviewed by Turco (1990)]. LPG is believed to be required for attachment of promastigotes to the epithelial cells that line the midgut of the sandfly (Davies et al., 1990). Following inoculation of the parasites by the sandfly, LPG promotes complement activation and resistance to complement-mediated damage in the bloodstream of the host (Puentes et al., 1988). LPG also plays a key role in the receptor-mediated attachment and entry into mammalian macrophages (Handman & Goding, 1984; Da Silva et al., 1989; Talamas-Rohana et al., 1990). Upon entry within host macrophages, LPG has been shown to be required for intracellular survival (Handman et al., 1986; Elhay et al., 1990; McNeely & Turco, 1990). The precise intracellular role (or roles) of LPG within phagolysosomes is unclear. There is evidence that the glycoconjugate may interact with the host cell's protein kinase C (McNeely & Turco, 1987; McNeely et al., 1989), thereby preventing activation of the microbicidal oxidative burst. LPG also might act as a chelator of divalent cations (i.e., $Ca^{2+}$ or $Fe^{2+}$) that are necessary to sustain the burst and/or behave as a scavenger of toxic oxygen metabolites (Chan et al., 1989; McNeely & Turco, 1990). Thus, the delineation of the three-dimensional structure of the glycan represents a major step in our understanding of the mechanism of LPG oligosaccharide–host molecule interactions. Furthermore, the demonstration that vaccination of mice with purified *Leishmania major* LPG induces resistance against cutaneous leishmaniasis (Handman & Mitchell, 1987; McConville et al., 1987) suggests that it might be possible to generate synthetic vaccines from structural homologues of LPG.

Here, by use of a combination of homo- and heteronuclear NMR spin coupling constant measurements together with restrained molecular mechanical minimization and molecular dynamics simulations, we have determined the structural and dynamic properties of the LPG from *L. donovani* and have investigated the effect of $Ca^{2+}$ ions on the 3D structure. The significance of these data is discussed in terms of the proposed biological role of this glycoconjugate.

## Experimental Procedures

*Purification of LPG.* LPG from *L. donovani* promastigotes was extracted and partially purified as described earlier

† Financial support was provided from The Wellcome Trust (S.W.H.), from UNDP/World Bank/WHO Special Programme for Research and Training in Tropical Diseases, and from NIH Grant AI20941 to S.J.T. S.J.T. is a Burroughs Wellcome Scholar in Molecular Parasitology.
‡ University of Dundee.
§ University of Kentucky Medical Center.

0006-2960/92/0431-654$03.00/0 

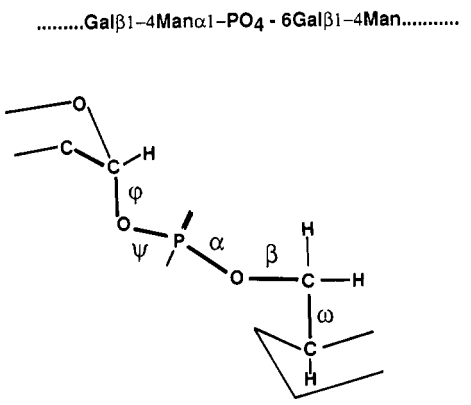


FIGURE 1: Definition of torsion angles in the Man$\alpha$1–$PO_4$–6Gal$\beta$ linkage. The bold lines indicate coupling pathways which give rise to heteronuclear couplings $J_{HP}$ and $J_{CP}$.

(Orlandi & Turco, 1987). The preparation was purified further by hydrophobic chromatography on phenyl-Sepharose (Turco et al., 1989).

*NMR Studies.* Material (27 mg) for NMR studies was prepared by passage through a small column of Chelex to remove cations, followed by flash evaporation and dissolution in 2.5 mL of 99.96% $D_2O$, followed by adjustment of the pH to 8.0 by addition of sodium hydroxide. Proton chemical shifts were referenced to internal acetone (2.225 ppm), phosphorus shifts were referenced to external phosphoric acid (0.0 ppm), and carbon shifts were referenced to external benzene (128.00 ppm). All spectra were recorded at a probe temperature of 300 K. $^1H$–$^1H$ COSY spectra (Ernst et al., 1987) were recorded with sweep widths of 1200 Hz in each dimension and with 64 scans per $t_1$ increment. A total of 512 increments were acquired, which after zero filling resulted in a data matrix of 1024 × 1024 real data points. Prior to two-dimensional Fourier transformation, data were apodized with sine bell resolution enhancement functions in each dimension. $^1H$–$^{13}C$ COSY spectra (Ernst et al., 1987) were recorded under similar conditions with a sweep width of 1200 Hz in the proton dimension and 7000 Hz in the carbon dimension and with 96 scans per $t_1$ increment.

## Energy Calculations

*Conventions.* Torsion angles for the Man$\alpha$1–$PO_4$–6Gal linkage are defined according to Figure 1. The glycosidic torsion angles $\varphi_1$ and $\psi_1$ for the Gal$\beta$1–4Man linkage are analogous to $\varphi_H$ and $\psi_H$ in IUPAC convention and are defined as H1–C1–O1–CX and C1–O1–CX–HX respectively, where HX and CX are aglyconic atoms. The torsion angle $\omega$ is similarly defined as H5–C5–C6–O6.

*Minimizations and Simulations.* All calculations were performed using the molecular mechanics package DISCOVER (Biosym Technologies Inc.) interfaced to a new parametrization of the AMBER force field (Weiner et al., 1984, 1986) for oligosaccharides (Homans, 1990). Oligosaccharide structures were created graphically using INSIGHT (Biosym Technologies Inc.), which provides a particularly convenient interface to DISCOVER.

(*a*) *Minimizations.* Energy minimization in vacuo was achieved by use of a quasi-Newton–Raphson algorithm (Fletcher & Powell, 1963), or by use of a steepest descents algorithm (Fletcher, 1980) in systems containing solvent, until the maximum derivative was less than 0.01 kcal/Å. Minimizations with explicit inclusion of solvent were performed by enclosure of the solute in a box 20 Å × 20 Å × 20 Å containing solvent water molecules and imposition of periodic boundary conditions using an orthogonal *P*1 (identity) space group. A nonbonded cutoff criterion of 10.0 Å was imposed, such that a pair of charge groups is added to the nonbonded pair list if the distance between switching atoms of each charge group is less than this distance. A fifth-order polynomial switching function was used to reduce smoothly the nonbonded potentials from full strength at an atom–atom distance of 6.5 Å to zero at an atom–atom distance of 8.5 Å. The nonbonded pair list was updated every 20 iterations.

(*b*) *Molecular Dynamics Simulations.* Molecular dynamics simulations with explicit inclusion of solvent were performed at constant pressure under conditions identical to those described for minimization. In each case the system was equilibrated with a thermal bath at 300 K with a coupling constant of 0.1 $ps^{-1}$. Simulations were run with a time step of 0.1 fs for 50 ps real-time. Equilibration was monitored empirically by observation of the total energy and was always complete within the first 10 ps. Data analysis was thus performed on the last 40 ps of each simulation by use of in-house written software. For this purpose, coordinates were stored periodically during the time course of the simulation. The minimum number of such coordinates required to represent adequately the conformational properties of the system during the time course was determined empirically.

(*c*) *Simulated Annealing.* Energy minimization by dynamical simulated annealing was achieved under conditions otherwise identical to those for molecular dynamics simulations, except that the system was equilibrated for 10 ps with a thermal bath at 300 K and thereafter recursively for 1 ps with a thermal bath 10 K lower in temperature until a final temperature of 10 K was obtained, giving a total simulation time of 39 ps. Following simulation for a further 1 ps at 5 K, the resulting geometry was minimized by use of a steepest descents algorithm until the maximum derivative was less than 0.01 kcal/Å.

*Force Field Parameters.* All atom types and parameters were as described (Homans, 1990), with the exception of certain parameters for the –Man$\alpha$1–$PO_4$–6Gal– linkage. New atom types were required for the definition of the phosphate group, and these were taken directly from AMBER (Weiner et al., 1984, 1986), together with appropriate charges. In addition, it was necessary to address the appropriate parametrization for the H1–C1–O1–P torsion term between mannose and the phosphate and for the H5–C5–C6–O6 torsion angle of galactose.

*H1–C1–O1–P Torsional Term.* In the previously described parametrization (Homans, 1990), an explicit torsional term is included to account for the exo-anomeric effect, i.e., the tendency of the torsional angle H1–C1–O1–CX in a glycosidic linkage (where CX is the aglyconic carbon) to exist in a preferred configuration depending upon anomeric and absolute configuration of the glycon. While the theoretical basis of this effect is not fully understood, it is known to involve electrostatic effects and/or delocalization resulting from electronic interactions between the ring oxygen and glycosidic oxygen of the glycon (Tvaroska & Bleha, 1989). Thus the nature of the substituent at CX does not influence the parametrization of the exo-anomeric torsional term per se, and the parameters previously defined for H1–C1–O1–CX are also applicable to H1–C1–O1–P.

*H5–C5–C6–O6 Torsional Term.* The nature of the parametrization described (Homans, 1990) is such that an explicit torsional term should not be necessary in order adequately to predict the preferred rotamer populations about the C5–C6 bond of monosaccharides. In order to confirm this, a grid search calculation was performed on methyl $\alpha$-D-galacto-

Table I: Values of Glycosidic Torsion Angles and Relative Energies during Simulated Annealing of Man$\alpha$1–$PO_4$–6Gal$\beta$1–4Man with Explicit Inclusion of Solvent

| | torsion angle (deg) | | | | | | | |
|---|---|---|---|---|---|---|---|---|
| structure | $\varphi$ | $\psi$ | $\omega$ | $\alpha$ | $\beta$ | $\varphi_1$ | $\psi_1$ | energy (kcal/mol) |
| initial | −51.99 | 179.87 | 62.09 | −179.91 | 179.69 | 50.47 | 1.58 | −48.82 |
| minimized | −47.50 | 169.57 | 53.94 | 172.08 | 174.95 | 53.30 | 9.17 | −1270.53 |
| annealed | −56.95 | 162.32 | 55.65 | −171.04 | −178.16 | 53.63 | 25.41 | −1635.48 |

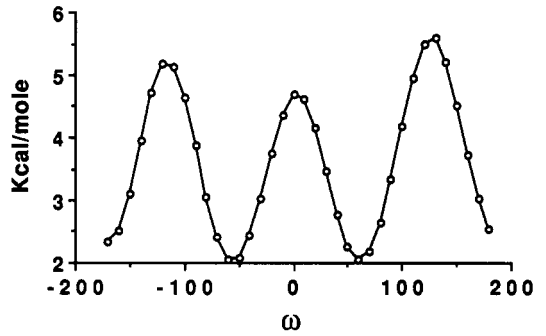


FIGURE 2: Plot of total energy vs $\omega$ for rotation about the C5–C6 bond of methyl $\alpha$-galactoside, resulting from an in vacuo calculation with a dielectric constant = 80.0 and parameters as described in the text.

pyranoside, by varying $\omega$ in 10° steps, followed by minimization at each step as described above, with a dielectric constant of 80.0 to simulate in part the effects of solvent water. The resulting energy profile is shown in Figure 2. Three minima were found at $\omega$ = +60°, −60°, and 180° with relative energies of 2.064, 2.040, and 2.527 kcal/mol, respectively, and these correspond with relative populations of 40%, 42%, and 18% at 300 K. The populations obtained experimentally by $^1$H NMR measurements on the same compound are 39 ± 2% (+60°), 47 ± 4% (−60°), and 14 ± 4% (180°) (Nishida et al., 1984), and thus the parametrization adequately predicts experimental data without further modification.

## Results

The lipophosphoglycan of *L. donovani* contains on average 16 Gal$\beta$1–4Man repeats, and simulation of a structure of this size is computationally intractable. Since explicit inclusion of solvent molecules for accurate simulation of the dynamic properties of oligosaccharides is essential (Homans, 1990), the size of molecule which can be simulated is further reduced. We therefore chose the smallest representative fragment of the lipophosphoglycan, namely, the trisaccharide Man$\alpha$1–$PO_4$–6Gal$\beta$1–4Man.

As an initial stage in the structure determination, the global minimum energy configuration of the trisaccharide was estimated with explicit inclusion of solvent. The fragment was solvated in a box 20 Å × 20 Å × 20 Å of solvent water molecules and was minimized by use of a steepest descents algorithm until the maximum derivative was less than 0.1 kcal/Å. The minimized structure was then subjected to simulated annealing as described above. The relative energies of the various geometries throughout this procedure together with the values of the glycosidic torsion angles are given in Table I.

The annealed structure by definition represents a static structure at zero Kelvin. At physiological temperatures, it has been adequately demonstrated that glycosidic linkages can map regions of conformational space around the global minimum which can be significant (Homans et al., 1987; Cumming & Carver, 1987; Imberty et al., 1989). In order to determine the regions of accessible conformational space about the global minimum which were available to the trisaccharide, the annealed structure was used as input to a 50-ps molecular dynamics simulation of the system at 300 K, as described above. The instantaneous values of each of the glycosidic torsion angles plotted over the last 40 ps of the simulation are shown in Figure 3. These suggest that the Gal$\beta$1–4Man linkage exists with restricted mobility, a result which is consistent with previous observations on similar glycosidic linkages. In contrast, there is significant freedom of motion about the Man$\alpha$1–$PO_4$–6Gal linkage. The presence of the phosphate allows this motion to be experimentally validated for certain torsion angles via heteronuclear coupling constants, as illustrated in Figure 1. The values of $\varphi$ can be validated by measurement of the $^3J_{HP}$ scalar coupling between the mannose C-1 proton and phosphate. This coupling (7.15 ± 0.3 Hz) was measured from the $^{31}$P spectrum of LPG with and without proton spin decoupling of the well-resolved mannose C-1 proton (Figure 4). By use of the Karplus equation appropriate for an H–C–O–P torsion (Lankhorst et al., 1984)

$$^3J_{HP} = 15.3 \cos^2 \theta - 6.1 \cos \theta + 1.6 \quad (1)$$

values of $\varphi$ consistent with this coupling were computed (Table II). In order to obtain additional constraints about this and other torsion angles, use was made of C–P coupling constants, for which the appropriate Karplus equation is (Lankhorst et al., 1984)

$$^3J_{CP} = 6.9 \cos^2 \theta - 3.4 \cos \theta + 0.7 \quad (2)$$

The C–P coupling constants could readily be measured from the proton-decoupled carbon spectrum (not shown) following assignment by conventional $^1$H–$^1$H and $^{13}$C–$^1$H correlated spectroscopy (Figure 5). Since eqs 1 and 2 are quadratic, there are in principle two solutions, and positive and negative values of each are consistent with the measured value of $J$ in view of the cosine function. In the case of C2–C1–O1–P, only one solution was possible. Since H1–C1–O1–P − 120° = C2–C1–O1–P, the only mutually consistent solution within error is $\varphi$ = −33.5°, (C2–C1–O1–P = −140.96°). This result

Table II: Spin Coupling Constants and Computed Torsion Angles for the Man$\alpha$1–$PO_4$–6Gal$\beta$ Fragment of the Intact Lipophosphoglycan of *L. donovani*

| torsion angle | $J$ (Hz) | computed angle (deg) |
|---|---|---|
| $\psi$ | | |
| H1–C1–O1–P | 7.15 ± 0.3 | ±33.5 (±2) |
| | | ±115.8 (±2) |
| C2–C1–O1–P | 7.5 ± 0.5 | ±140.96 (±4) |
| $\beta$ | | |
| H6–C6–O6–P | 6.8 ± 0.3 | +60.0 (25.3 ± 7%) |
| H6′–C6–O6–P | 8.8 ± 0.3 | −60.0 (14.7 ± 7%) |
| | | 180.0 (60.0 ± 7%) |
| H6–C6–O6–P | 8.8 ± 0.3 | +60.0 (14.7 ± 7%) |
| H6′–C6–O6–P | 6.8 ± 0.3 | −60.0 (25.3 ± 7%) |
| | | 180.0 (60.0 ± 7%) |
| $\omega$ | | |
| H5–C5–O6–H6 | 7.0 ± 0.5 | −60.0 (42.7 ± 7%) |
| H5–C5–O6–H6′ | 5.0 ± 0.5 | +60.0 (29.8 ± 7%) |
| | | 180.0 (27.5 ± 7%) |
| H5–C5–O6–H6 | 5.0 ± 0.5 | −60.0 (12.9 ● 7%) |
| H5–C5–O6–H6′ | 7.0 ± 0.5 | +60.0 (53.1 ± 7%) |
| | | 180.0 (34.0 ± 7%) |

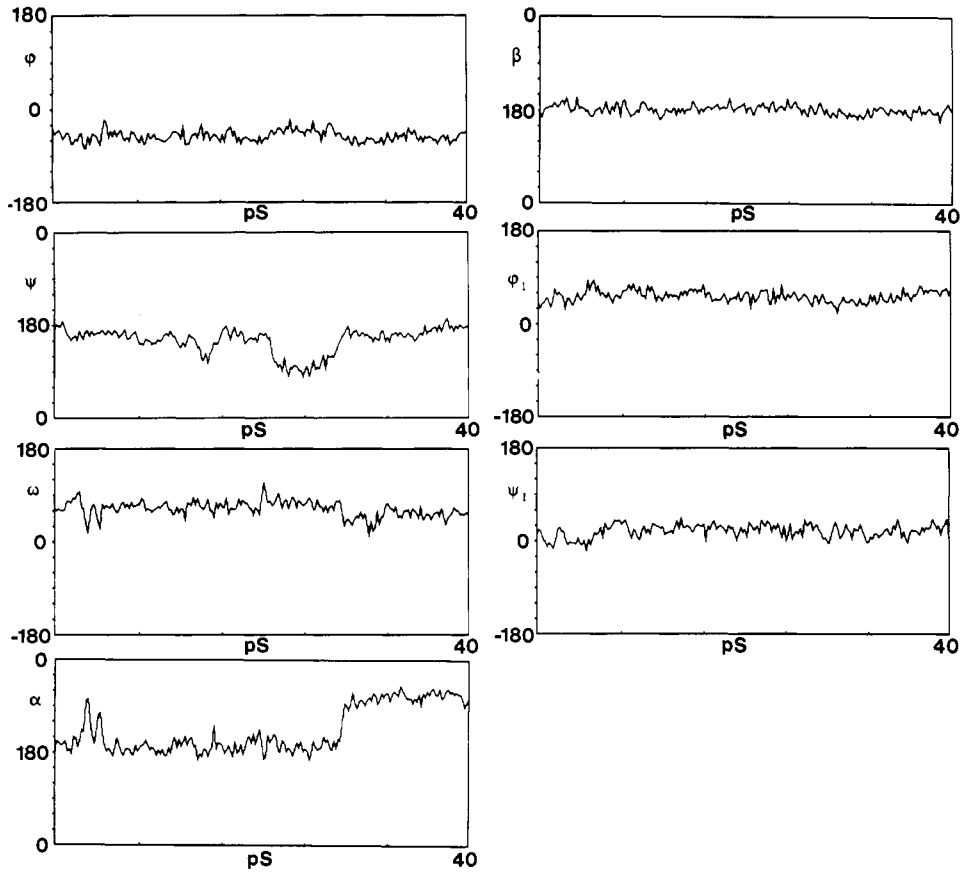


FIGURE 3: Time evolution of the torsion angles defined in Figure 1 during a 40-ps MD simulation of Man$\alpha$1–$PO_4$–6Gal$\beta$1–4Man with explicit inclusion of $H_2O$. See text for details.

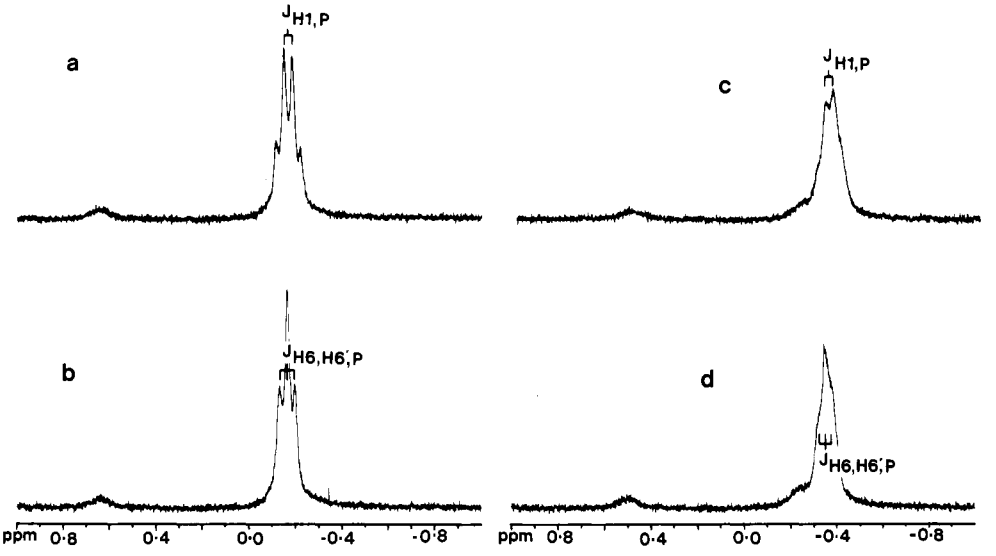


FIGURE 4: $^{31}P$ NMR spectra of the intact lipophosphoglycan of *L. donovani*. (a) Undecoupled spectrum in the absence of $Ca^{2+}$; (b) spectrum recorded with decoupling of the mannose C-1 proton; (c,d) as (a) and (b), respectively, in the presence of $Ca^{2+}$ equimolar with the concentration of intrinsic phosphate. The relevant spin coupling constants can be measured as shown.

is in reasonable agreement with the average value of $\varphi$ (−51.93°) over the 40-ps MD simulation of the trisaccharide. The discrepancy probably derives from the fact that eqs 1 and 2 are parametrized for HCOP and CCOP fragments in nucleic acids rather than glycosidic linkages and will be less accurate in application to the latter in view of the electronegativity of the ring oxygen.

In similar fashion to the above, the values of $\beta$ can be validated by measurement of the $^3J_{HP}$ scalar coupling between each geminal C-6 proton of galactose and phosphate. In this case it is necessary to consider the formal possibility that the value of $\beta$ can adopt values defining three stable rotamers, 60°, −60°, and 180°, which correspond in turn to the three staggered conformations about the C6–O6 bond. Since the predicted values of $J$ for each of these rotamers can be computed from eq 1, and since $J_{H6-P}$ and $J_{H6'-P}$ can be measured from the phosphorus spectrum (Figure 4a,b), then the relative populations of the three rotamers can be computed with the normalization condition that their sum must equal 100%. In the absence of *stereospecific* assignments for H6 and H6′, two formal solutions must be considered (Table II). From these solutions it is possible to predict the value of $J_{C5-P}$ from eq 2,

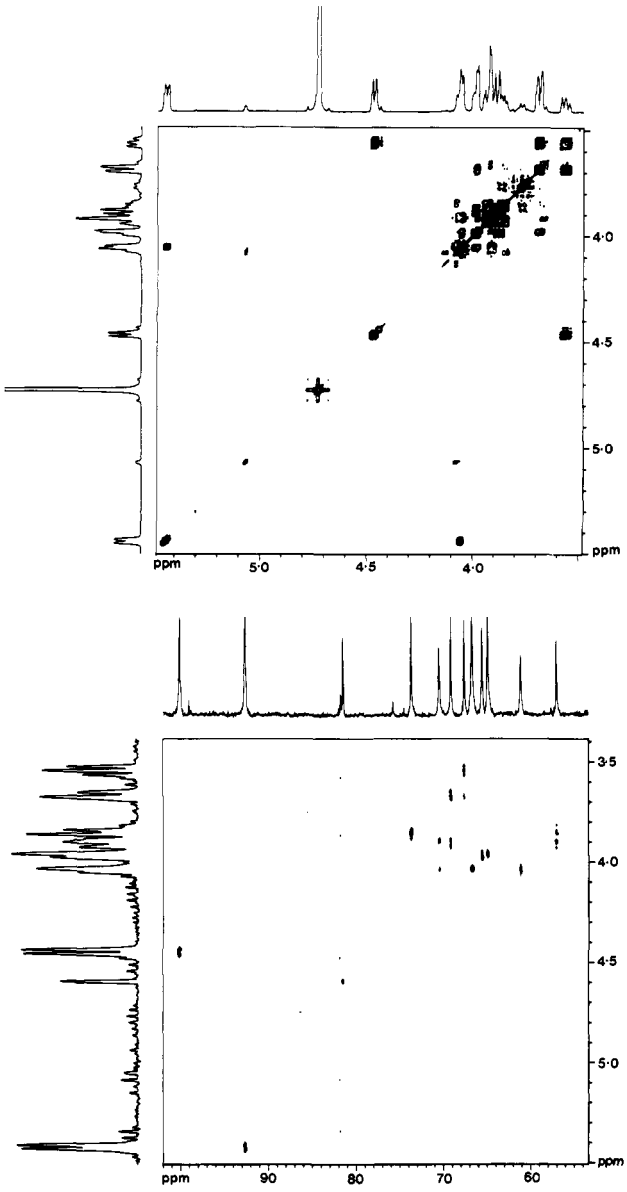


FIGURE 5: (Top) $^1H$–$^1H$ COSY and (bottom) $^1H$–$^{13}C$ COSY spectra of the intact lipophosphoglycan of *L. donovani*.

since this is sensitive to the torsion angle C5–C6–O6–P. The predicted value of this coupling is 7.2 Hz in each case, compared with a measured value of 8.1 ± 0.5 Hz. While it is not possible from this result to distinguish between the two possible solutions, the agreement between the predicted and measured values of $J_{C5-P}$ is reasonable. Notably, each solution predicts that the $\beta$ = 180° conformer is dominant. The value of $\beta$ over the time course of the 40-ps MD simulation of the trisaccharide is indeed restricted to this region of conformational space. However, no torsional transitions are observed, indicating that while such transitions are fast on the NMR time scale, the rate of interconversion is greater than 40 $ps^{-1}$ and a very much longer MD simulation is required in order to observe these transitions.

The rotamer distributions about the torsion angle $\omega$ can be determined from the measured values of $J_{H5-H6}$ and $J_{H5-H6'}$ (Brisson & Carver 1983; Homans et al., 1986). Determination of these coupling constants is, however, complicated by the virtual degeneracy of the chemical shifts of Gal$\beta$1 H6 and H6′. These were thus measured from the cross peak correlating H5 with the H6's in a double-quantum-filtered COSY spectrum of LPG (not shown). These values are given in Table II. From these, the relative populations of rotamers can be computed by use of the appropriate Karplus relationship as described by Ohrui et al. (1985). Again, in the absence of stereospecific assignments, two solutions must be formally considered. However, by use of stereospecific deuteration, Ohrui et al. (1985) demonstrated that the dominant rotamer in galacto-configuration residues is $\omega$ = −60°, suggesting that the first solution in Table II is correct. In contrast, the 40-ps MD simulation of the trisaccharide suggests that $\omega$ = +60°. However, within experimental error (Table II), the populations of the $\omega$ = −60° and $\omega$ = +60° rotamers may be identical. Under these circumstances, the simulated annealing strategy will not distinguish between these rotamers since the population probabilities are essentially identical. While, therefore, both of these rotamers should in principle be observed during the course of the MD simulation, such conformational transitions will be relatively infrequent due to the significant energy barrier to rotation (Figure 1), and an MD simulation very much greater than 40 ps would be required in order to observe the conformational space mapped by $\omega$ in an adequate manner.

The absence of spin couplings sensitive to the torsion angles $\alpha$ and $\psi$ prevents experimental investigation of the conformational space mapped by these. The MD simulation of the trisaccharide indicates that $\psi$ interconverts between 180° and 60°, whereas $\alpha$ interconverts between 180° and −60°. However, in view of the limited length of the MD simulation, the possible existence of the rotamers $\psi$ = −60° and $\alpha$ = 60° cannot be excluded.

From the above it is clear that the number of possible conformational states about the Man$\alpha$1–$PO_4$–6Gal$\beta$ linkage is large. In order to investigate the influence of these states on the overall conformation of a larger fragment more representative of intact LPG, only the major conformers about the Man$\alpha$1–$PO_4$–6Gal$\beta$ linkage were considered further: A series of tetramers [Gal$\beta$1–4Man$\alpha$1–$PO_4$–6]$_4$ were constructed manually by graphical procedures with all values of $\psi$ and all values of $\alpha$ in each adjusted to either 60°, −60°, or 180°, giving a total of nine structures. This ensemble is necessary in view of the absence of experimental data defining the relative rotamer populations about $\psi$ and $\alpha$. Each of these structures was subjected to energy minimization with the values of $\varphi$, $\omega$, and $\beta$ restrained to the experimentally defined major conformer, i.e., $\varphi$ = −33.5°, $\omega$ = −60°, and $\beta$ = 180°. In each case harmonic constraints were applied with a weak (5-kcal) force constant. For computational tractability, these minimizations were computed in vacuo with a dielectric constant = 80.0 to simulate in part the effects of solvent. While in principle this may lead to significant deviations from the potential surface computed with explicit inclusion of solvent, previous observations suggest that the minimum energy configuration can be obtained with good accuracy by use of this approach (Homans, 1990). This gave rise to eight minimized structures (Figure 6), and the relevant values of $\varphi$, $\psi$, $\omega$, $\alpha$, $\beta$, $\varphi_1$, and $\psi_1$ are shown in Table III. The structure corresponding to $\psi$ = −60, $\alpha$ = 180.0 did not converge during minimization due to band van der Waals contacts and was thus excluded as a major conformer.

The effect of $Ca^{2+}$ upon the 3D structure of the glycan was determined experimentally by addition of $CaCl_2$ at a concentration equimolar with the concentration of phosphate, with readjustment of the pH to 8.0. While the phosphorus resonance was broadened and shifted by $Ca^{2+}$ (Figure 4c,d), the magnitudes of the scalar coupling constants $J_{H1-P}$ and $J_{H6-P}$ were not significantly perturbed in comparison with those measured in the absence of $Ca^{2+}$ ($J_{H1-P}$ = 6.1 ± 0.4 Hz, $J_{H6-P}$

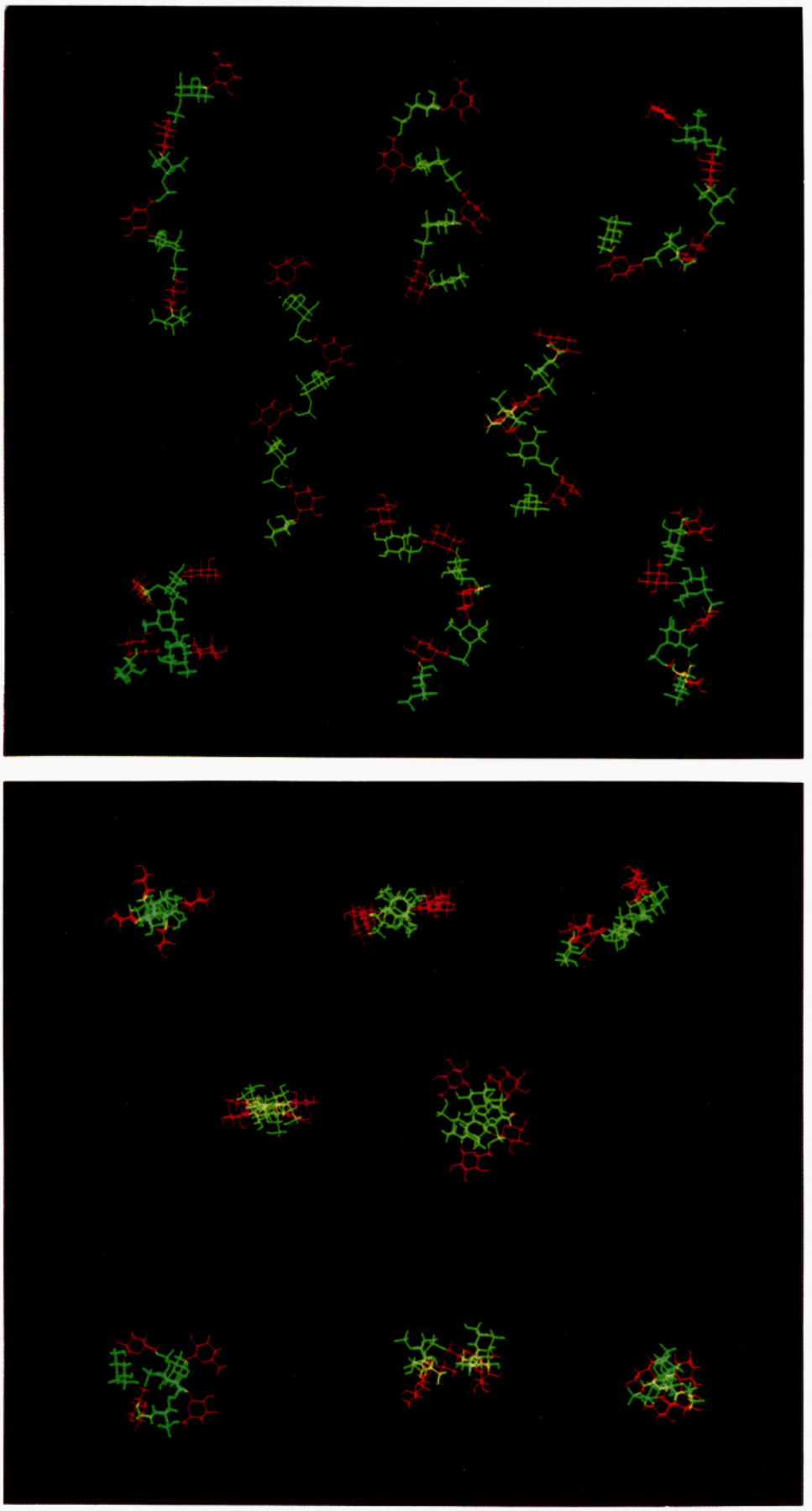

FIGURE 6: Eight energy-minimized structures of [Gal$\beta$1–4Man$\alpha$1–$PO_4$–6]$_4$, corresponding with structures 1–8 in Table III, viewed (top) longitudinally and (bottom) down the long axis of the repeats. The structures in each figure are as follows: top row (left to right), structures 1, 2, and 3; middle row, structures 4 and 5; bottom row, structures 6, 7, and 9. Structure 8, which showed no convergence during energy minimization, is not shown. Galactose residues are colored red, and mannose residues are colored green.

Table III: Initial and Final Energies and Torsion Angles for Nine Geometries of [Galβ1–4Manα1–$PO_4$–6]$_4$[a]

| structure | initial energy (kcal/mol) | permutation ψ | permutation α | final energy (kcal/mol) | torsion values for minimized conformers (deg) φ | ψ | α | β | ω | $\varphi_1$ | $\psi_1$ |
|---|---|---|---|---|---|---|---|---|---|---|---|
| 1 | 31.34 | 180 | −60 | 1.60 | | | | | | 54.2 | 16.7 |
| | | | | | −43.8 | 174.3 | −62.5 | 177.7 | −44.1 | 55.5 | 19.6 |
| | | | | | −44.0 | 172.9 | −64.5 | −178.4 | −46.4 | 53.9 | 16.9 |
| | | | | | −43.5 | 173.9 | −62.6 | 178.0 | −44.3 | 55.8 | 18.5 |
| 2 | 93.34 | 180 | 180 | 7.15 | | | | | | 53.1 | 18.4 |
| | | | | | −43.5 | 170.9 | −172.3 | 174.8 | −50.0 | 55.1 | 20.7 |
| | | | | | −47.0 | 167.9 | −170.8 | 175.4 | −49.4 | 52.7 | 18.4 |
| | | | | | −43.7 | 170.8 | −172.3 | 174.8 | −50.0 | 55.4 | 20.0 |
| 3 | 87.63 | 180 | 60 | 1.74 | | | | | | 53.4 | 17.2 |
| | | | | | −43.1 | 171.9 | 67.9 | 173.7 | −52.1 | 54.4 | 19.7 |
| | | | | | −46.0 | 169.3 | 70.7 | 169.3 | −51.3 | 52.9 | 17.0 |
| | | | | | −43.0 | 172.0 | 67.8 | 173.7 | −52.2 | 54.3 | 20.6 |
| 4 | 3621.0 | 60 | −60 | 9.95 | | | | | | 51.6 | 20.2 |
| | | | | | −36.6 | 77.9 | −63.3 | 178.6 | −51.3 | 51.9 | 21.2 |
| | | | | | −29.1 | 75.2 | −56.7 | −179.0 | −52.8 | 53.6 | 20.6 |
| | | | | | −37.2 | 78.1 | −62.7 | 178.7 | −52.0 | 52.3 | 20.1 |
| 5 | 78.64 | 60 | 180 | −1.39 | | | | | | 54.5 | 17.4 |
| | | | | | −42.2 | 66.0 | 179.5 | 178.4 | −49.9 | 56.9 | 18.1 |
| | | | | | −40.2 | 62.3 | −176.7 | 177.3 | −49.6 | 54.8 | 16.2 |
| | | | | | −42.6 | 66.2 | 179.4 | 178.1 | −50.0 | 56.8 | 18.6 |
| 6 | 70.54 | 60 | 60 | 9.65 | | | | | | 54.5 | 18.3 |
| | | | | | −43.2 | 69.9 | 61.2 | 177.3 | −53.2 | 55.8 | 18.7 |
| | | | | | −42.1 | 66.8 | 62.4 | −179.5 | −51.4 | 54.8 | 18.3 |
| | | | | | −43.5 | 69.9 | 61.1 | 177.1 | −53.2 | 55.6 | 18.4 |
| 7 | 85.95 | −60 | −60 | 13.94 | | | | | | 55.4 | 21.8 |
| | | | | | −34.6 | −59.4 | −70.6 | 177.6 | −46.3 | 57.2 | 23.5 |
| | | | | | −36.5 | −57.9 | −74.3 | 172.3 | −51.2 | 54.7 | 21.4 |
| | | | | | −34.5 | −59.3 | −70.4 | 177.8 | −46.3 | 57.0 | 23.3 |
| 8 | $>10^4$ | −60 | 180 | *b* | | | | | | | |
| 9 | 1419.60 | −60 | 60 | 30.21 | | | | | | 53.0 | 26.5 |
| | | | | | −35.7 | −57.6 | 78.5 | 175.4 | −67.2 | 54.7 | 29.5 |
| | | | | | −38.0 | −55.1 | 80.0 | 179.4 | −76.2 | 55.0 | 29.3 |
| | | | | | −34.9 | −58.9 | 78.0 | 176.2 | −68.0 | 54.8 | 26.9 |

[a] See text for details. [b] No convergence.

= 6.5 ± 0.4 and 8.2 ± 0.4 Hz). Similarly, the couplings $J_{C2-P}$ and $J_{C5-P}$ were not significantly perturbed ($J_{C2-P}$ = 7.4 ± 0.5 Hz, $J_{C5-P}$ = 7.5 ± 0.5 Hz). These data suggest that $Ca^{2+}$ does not perturb the overall three-dimensional structure of the glycan, although the broadening and shift of the phosphorus resonance indicate that $Ca^{2+}$ binds to LPG in the vicinity of the phosphate.

## Discussion

The data above indicate that the LPG exists in solution with significant mobility about the Manα1–$PO_4$–6Galβ linkage. In view of the absence of nuclear Overhauser effect data across this linkage, and with limited homonuclear and heteronuclear spin coupling constant measurements, only limited experimental data are available with which to characterize this mobility. Nevertheless, the available experimental data, when combined with theoretical predictions in the form of restrained minimization, predict a total of eight major stable structures for the LPG molecule, each derived from a particular stable rotamer about ψ and α. The final energies of the eight minimized structures are low (Table III), indicating that each structure may contribute to the ensemble of conformers at physiological temperature. Since the MD simulations suggest that transitions between stable rotamers about ψ and α occur at physiological temperatures, these conformers will constantly interchange with each other under these conditions. The relative populations will partition according to the Boltzmann law, with structure 5 as the preferred conformer, closely followed by structures 1 and 3. Structures 2, 4, 6, 7, and 9 all have significantly higher energies, and hence the relative occupancy of these conformers will be significantly lower at physiological temperatures. The conformational invariance of LPG in the presence or absence of $Ca^{2+}$ rules out the possibility that this cation may act as a conformational switch. However, the demonstrable binding of $Ca^{2+}$ to LPG is consistent with a role as a scavenger of intracellular $Ca^{2+}$.

An intriguing feature of each of the low-energy conformers is that the C-3 hydroxyl of each galactose residue is exposed and freely accessible. Notably, the –$PO_4$–Galβ1–4Manα1– repeat units are substituted at this position either with glucose, or with galactose and arabinose in the LPGs from *Leishmania mexicana* (Ilg et al., 1991) and *L. major* (McConville et al., 1990), respectively. These additional units could thus be accommodated without major conformational changes to the repeat backbone. The presence of such common conformational properties between the LPGs of various species provides a possible explanation for the existence of a monoclonal antibody (WIC108) which recognizes LPG from all species. Conversely, the side chains are probably the epitopes recognized by monoclonal antibodies which are species-specific in terms of LPG recognition, such as the WIC79.3 monoclonal antibody specific for the LPG of *L. major*.

While we have chosen to model a series of conformers, each with the same configuration about the Manα1–$PO_4$–6Galβ linkage, clearly there is no energetic requirement for such concerted dynamics, and each Manα1–$PO_4$–6Galβ linkage may exist in a different configuration within the same LPG molecule. These torsional oscillations confer an ability upon the LPG molecule to contract or expand, resulting in a molecule whose length is potentially 90 Å when fully contracted and 160 Å when fully extended, assuming an average of 16 repeats.

The extended form may even be more prominent in view of recent findings showing that the LPG from virulent leishmania possesses approximately double the number of repeat units compared to the average 16 units present in LPG from

noninfectious parasites (Sacks et al., 1990). The potential biological significance of this extension–contraction behavior is unclear at present but may involve specific interactions of the glycan with lectin-like molecules in the sandfly's midgut (Davies et al., 1990), the third component of complement (Puentes et al., 1988), and the "lectin-like lipopolysaccharide" binding site present on the CD18 family of macrophage surface receptors, CR3, LFA-1, and p150-95 (Talamas-Rohana et al., 1990).

Another possible significance of the model is that it may assist in efficient packing of the LPG molecules on the promastigote surface, affording protection in the various hydrolytic environments the parasite encounters in its life cycle. The copy number of LPG is (1.3–5.0) × $10^6$ molecules/cell (Orlandi & Turco, 1987; McConville & Bacic, 1989), and the cross-sectional area of, for example, structure 1 when viewed perpendicular to the membrane is ~3.4 $nm^2$. Thus, the computed coverage afforded by LPG (4.4–17 $\mu m^2$), compared with the computed surface area of *Leishmania* parasites, which is ~27 $\mu m^2$, suggests that LPG may cover a significant proportion, if not all, of the plasma membrane. These estimates are consistent with recent electron microscopic studies of the promastigote surface, which have revealed the presence of densely packed filamentous structures on freeze–fracture preparations (Plimenta et al., 1989).

The mobility of the Man$\alpha$1–$PO_4$–6Gal$\beta$ linkage will additionally confer significant configurational entropy on the LPG molecule. On binding to a putative receptor, this entropy will be lost at the expense of binding energy. However, the rate constant for binding to the receptor ($k_{on}$) will be enhanced, which may thus be of importance in macrophage invasion. This mobility may, however, prove problematic in the design of molecular mimics of LPG, since the precise geometry recognized by an antibody cannot readily be predicted, and hence it would be necessary to design a mimic which both has the same geometry and maps the same conformational space as the native LPG molecule. Under these circumstances it will perhaps prove simpler to focus attention upon organic synthesis of the LPG repeat units per se as potential vaccines.

## References


Brisson, J.-R., & Carver, J. P. (1983) *Biochemistry 22*, 3680.

Chan, J., Fujiwara, T., Brennan, P., McNeil, M., Turco, S. J., Sibille, J., Snapper, M., Aisen, P., & Bloom, B. R. (1989) *Proc. Natl. Acad. Sci. U.S.A. 86*, 2453.

Cumming, D. A., & Carver, J. P. (1987) *Biochemistry 26*, 6664.

Da Silva, R. P., Hall, B. F., Joiner, K. A., & Sacks, D. L. (1969) *J. Immunol. 143*, 617.

Davies, C. R., Cooper, A. M., Peacock, C., Lane, R. P., & Blackwell, J. M. (1990) *Parasitology 101*, 337.

Eilam, Y., El-On, J., & Spina, D. T. (1985) *Exp. Parasitol. 59*, 161.

Ernst, R. R., Bodenhausen, G., & Wokaun, A. A. (1987) *Principles of NMR in One and Two Dimensions*, Clarendon Press, Oxford, U.K.

Fletcher, R. (1980) Unconstrained Optimisation, *Practical Methods of Optimisation*, Vol. 1, Wiley and Sons, Chichester, U.K.

Fletcher, R., & Powell, M. J. D. (1963) *Comput. J. 36*, 163.

Handman, E., & Goding, J. W. (1984) *EMBO J. 4*, 329.

Handman, E., & Mitchell, G. F. (1985) *Proc. Natl. Acad. Sci. U.S.A. 82*, 5910.

Handman, E., Greenblatt, C. L., & Goding, J. W. (1984) *EMBO J. 3*, 2301.

Handman, E., Schnur, L. F., Spithill, T. W., & Mitchell, G. F. (1986) *J. Immunol. 137*, 3608.

Hernandez, A. G. (1983) in *Cytopathology of Parasitic Diseases*, CIBA Foundation Symposium 99, pp 138–156, Pitman Books Ltd., London.

Homans, S. W. (1990) *Biochemistry 29*, 9110.

Homans, S. W., Dwek, R. A., Boyd, J., Mahmoudian, M., Richards, W. G., & Rademacher, T. W. (1986) *Biochemistry 25*, 6342.

Homans, S. W., Pastore, A., Dwek, R. A., & Rademacher, T. W. (1987) *Biochemistry 26*, 6649.

Ilg, T., Etges, R., Overath, P., Thomas-Oates, J., McConville, M. J., Homans, S. W., & Ferguson, M. A. J. (1991) *J. Biol. Chem.* (submitted for publication).

Imberty, A., Tran, V., & Perez, S. (1990) *J. Comput. Chem. 11*, 205.

King, D. L., Chang, Y., & Turco, S. J. (1987) *Mol. Biochem. Parasitol. 24*, 47.

Lankhorst, P. P., Haasnoot, C. A. G., Erkelens, C., & Altona, C. (1984) *J. Biomol. Struct. Dyn. 1*, 1387.

McConville, M. J., & Bacic, A. (1990) *Mol. Biochem. Parasitol. 38*, 57.

McConville, M. J., Bacic, A., Mitchell, G. F. & Handman, E. (1987) *Proc. Natl. Acad. Sci. U.S.A. 84*, 8941.

McConville, M. J., Thomas-Oates, J. E., Ferguson, M. A. J., & Homans, S. W. (1990) *J. Biol. Chem. 265*, 19611.

McNeely, T. B., & Turco, S. J. (1987) *Biochem. Biophys. Res. Commun. 148*, 653.

McNeely, T. B., & Turco, S. J. (1990) *J. Immunol. 144*, 2745.

McNeely, T. B., Rosen, G., Londner, M. V., & Turco, S. J. (1989) *Biochem. J. 259*, 601.

Nishida, Y., Ohrui, H., & Meguro, H. (1984) *Tetrahedron Lett. 25*, 1575.

Ohrui, H., Nishida, Y., Watanabe, M., Hori, H., & Meguro, H. (1985) *Tetrahedron Lett. 26*, 3251.

Orlandi, P. A., & Turco, S. J. (1987) *J. Biol. Chem. 262*, 10384.

Pimenta, P. F., da Silva, R. P., Sacks, D. L., & da Silva, P. (1989) *Eur. J. Cell Biol. 48*, 180.

Puentes, S. M., Sacks, D. L., da Silva, R. P., & Joiner, K. A. (1988) *J. Exp. Med. 167*, 887.

Russell, D. G., & Wright, S. D. (1988) *J. Exp. Med. 168*, 279.

Sacks, D. L., Brodin, T., & Turco, S. J. (1990) *Mol. Biochem. Parasitol. 42*, 225.

Talamas-Rohana, P., Wright, S. D., Lennartz, M. R., & Russell, D. G. (1990) *J. Immunol. 144*, 4817.

Turco, S. J. (1990) *Exp. Parasitol. 70*, 241.

Turco, S. J., Hull, S. R., Orlandi, P. A., Sheperd, S. D., Homans, S. W., Dwek, R. A., & Rademacher, T. W. (1987) *Biochemistry 26*, 6233.

Turco, S. J., Orlandi, P. A., Jr., Homans, S. W., Ferguson, M. A. J., Dwek, R. A., & Rademacher, T. W. (1989) *J. Biol. Chem. 264*, 6711.

Tvaroska, I., & Bleha, T. (1989) *Adv. Carbohydr. Chem. Biochem. 47*, 45.